Kinetics of the Dissolution of Alumina in Acidic Solution in a Flow System

The kinetics of dissolution of alumina in aqueous solutions of H_2SO_4 was studied at ambient temperature under continuous-flow conditions. The results are consistent with a model involving rapid hydration of the surface, adsorption-desorption of H^+ to form precursor sites, and rate-determining parallel reactions of the precursor sites to form dissolved aluminum and an insoluble surface species. The model also involves renewal of a precursor site after each dissolution step.

The adsorption-desorption of H^+ was represented by a Langmuir isotherm. The dissolution data were correlated by a kinetic equation that was developed by assuming the dissolution step is first order in precursor concentration, and the deactivation step is second order in precursor concentration.

Myles D. Crawford, Jerry Baumgart, Mahnoosh Shoaei, William R. Ernst
School of Chemical Engineering
Georgia Institute of Technology
Atlanta, GA 30332-0100

Introduction

The interaction of metal oxides with inorganic acids is encountered in many engineering problems—for example, hydrometallurgical processing (Dutrizac and MacDonald, 1974), semiconductor manufacture (Grabmaier, 1982), catalyst preparation (Maatman et al., 1971; Santacesaria et al., 1977; Shyr and Ernst, 1980), catalyst regeneration, (Hernandez, 1982; Ganguli, 1984; Myerson and Ernst, 1985), and acid rain pollution (Mandelbaum, 1984).

All of these problems involve the modification of solid surfaces by acid. It is desirable in most of these problems to prevent damage to the basic structure of the solid by limiting the time of contact between the acid and the surface or by protecting the surface by other means. It is therefore of interest to gain a better understanding of the early stages in the contacting of metal oxides and acids.

The purpose of this work was to examine the dissolution of alumina in aqueous acid solutions. Many authors (Hulbert and Huff, 1970; Kabai, 1973; Gorichev et al., 1976; Diggle et al., 1970; Warren and Devuyst, 1974; Franke et al., 1987) have studied the kinetics of dissolution of alumina by inorganic acids in a batch system. In several of these studies the batch data could not be fitted by conventional power law kinetic models or diffusion-reaction models. An equation based upon a nucleation process (Christian, 1965) was used successfully in correlating batch dissolution data for over 50 metal oxide systems, although there is no sound theoretical basis for applying this model to a dissolution process.

These previous studies have shown that the dissolution process usually involves a competing process which lowers the rate of dissolution with time. Some of these authors have suggested reaction sequences to explain the dissolution process for metal oxides, which for alumina has the following stoichiometry:

$$Al_2O_3 + 6H^+ \rightarrow 2Al^{3+} + 3H_2O \qquad (1)$$

They agree that the process is complex and speculate on the types of surface and solution ions that are involved. Although proposed sequences may differ in detail, they generally involve initial rapid hydration of the alumina surface followed by rapid equilibration by adsorbing hydrogen ions. Both processes are followed by a dissolution step or further attack of the surface by species in solution. Some authors have suggested steps involving formation of insoluble species to explain why dissolution rate generally decreases with time.

The work of Franke (1985) and Franke et al. (1987) for batch dissolution of Al_2O_3 in H_2SO_4 solutions can be qualitatively explained by such a sequence. In general, however, batch dissolution data may be difficult to interpret, especially if several time-dependent steps occur simultaneously. Continuous-flow experiments may provide more definitive information about the dissolution process by eliminating the time dependence of one or more of the variables. The geological literature contains many examples of kinetic studies using flow reactors for dissolution of minerals containing alumina (Holdren and Speyer, 1985; Chou

Correspondence concerning this paper should be addressed to W. R. Ernst.

and Wollast, 1985). These studies usually involve mineral samples with low surface areas (<100 m^2/kg) and reactors with high space times.

The purpose of this study was to examine the initial stages of dissolution of high surface area alumina in a continuous-flow, packed-bed reactor with low space time, and to attempt to explain the results in terms of a simple kinetic model that includes the general features observed by previous authors.

Experimental Method

Continuous-flow experiments were conducted by passing sulfuric acid solutions of various concentrations through a packed bed of alumina particles in a tube at ambient temperature. Alcoa F-1 alumina was used throughout the study. Alcoa reported a BET surface area of 2.5×10^5 m^2/kg and a pore volume of 4×10^{-4} m^3/kg. The large surface area is due primarily to internal pores. The external surface area is insignificant compared to the total. The alumina was crushed, screened to a 16–20 mesh size range, and dried in a 393 K oven for at least 24 h before it was used in the kinetics experiments.

Weighed samples of crushed alumina (1×10^{-3} kg) were packed on top of a coarse fritted glass disc inside a Pyrex tube, Figure 1. A plug of glass wool was placed at the top of the bed. The approximate bed dimensions were 9.5×10^{-3} m dia by 1.3×10^{-2} m length.

Before a kinetics experiment was begun, deionized water was passed through the bed for about 15 min in order to wet the alumina surface; the interstitial water was then removed by draining the bed and passing air through it. For the kinetics experiments, a peristaltic pump was used to maintain a constant flow rate of acid through the bed. A timer was started when the first drop of liquid was observed to drain from the bottom of the bed. The ranges of flow rates and H_2SO_4 feed concentrations were respectively 0.25×10^{-6} to 1.5×10^{-6} m^3/s and 0.0625 to 10 v/v %. Approximate space time in the reactor ranged from 0.6 to 3.7 m^3 bed × s/m^3 liquid.

Samples of the liquid effluent were collected in Nalgene bottles for aluminum analysis. Aluminum concentrations were determined with a Perkin Elmer 2380 atomic absorption spectrophotometer, operating with a nitrous oxide-acetylene flame at a wavelength of 309.3 nm and a slit width of 0.7 nm.

Three experiments identical in procedure to that of the above series were run to determine changes in pH of the effluent with time on stream. The flow rate in each run was 1×10^{-6} m^3/s.

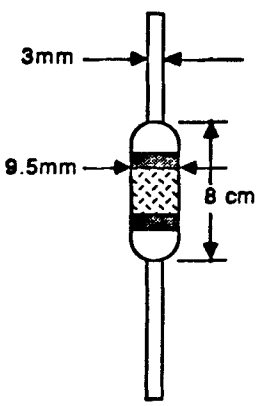

Figure 1. Packed alumina bed, tube dimensions.

The pH values of the feed solutions spanned those used in the above series. The pH measurements were made within several seconds after the samples were collected. Table 1 shows that pH did not vary with time on stream, and that pH values of effluent samples were about equal to those of feed solution.

The reaction rate (kg Al/s · kg bed) was determined from the sample concentration, flow rate of acid solution, and weight of the bed:

$$\text{Rate} = \frac{C \times F}{W} \tag{2}$$

This equation was developed by assuming that the bed is a differential reactor. This assumption is justified since only a negligible fraction of the aluminum in the bed is dissolved as the liquid passes through it and since the fractional conversion of H_2SO_4 is negligible, as shown in Table 1.

BET surface areas of alumina samples were measured after dissolution experiments by a continuous-flow technique in a Micromeritics Pulse ChemiSorb 2700 adsorption apparatus. This technique involved measuring the uptake of N_2 from a flowing stream of N_2-He mixture. The measurement was made at liquid N_2 temperature. This instrument provided rapid surface area measurements which we found to agree well with measurements in a standard volumetric apparatus.

Model Development

We began a search for the simplest mathematical model that would describe continuous-flow dissolution results and would incorporate the qualitative features of previously published mechanisms. The alumina surface was assumed to consist of a fixed number (n_T) of sites, all of which were rapidly converted to hydrated sites, X, during the prewetting process. We used the following sequence of steps to represent the disposition of the aluminum species during the dissolution process.

$$X \underset{-H^+}{\overset{+H^+}{\rightleftharpoons}} X^* \tag{3}$$

$$X^* \longrightarrow P \tag{4}$$

$$X^* \searrow D\downarrow \tag{5}$$

Rapid hydrogen ion adsorption-desorption equilibrium, Eq. 3, to form a number, s_o, of precursor sites, X^*, was assumed to occur when acid was introduced. Therefore, at the early stages of each experiment the surface consisted only of s_o X^* sites and ($n_T - s_o$) X sites. Assuming Eq. 3 is elementary and involves one

Table 1. pH of H_2SO_4 Solutions During Continuous-Flow Dissolution Experiments

Sample Time s	pH		
	Run A	Run B	Run C
3–10	1.72	0.93	−0.21
35–65	1.72	0.93	−0.21
115–125	1.73	0.93	−0.21
1,000–1,010	1.73	0.93	−0.22
Feed	1.72	0.93	−0.21

hydrogen ion per site leads to the Langmuir expression:

$$s_o = \frac{n_T K_a[H^+]}{1 + K_a[H^+]} \tag{6}$$

The rate-determining steps were assumed to be represented by Eqs. 4 and 5, where P is a solubilized aluminum species and D is a deactivated (insoluble) surface site. These steps may involve interaction of X^* sites with species in solution such as H^+ and SO_4^- (Diggle et al., 1970).

The deactivation process, Eq. 5, would cause the surface composition of the alumina to vary, since the number of X and X^* sites would decline with time as some sites deactivated. At t, the surface was considered to consist of s X^* sites, d D sites, and $(n_T - s - d)$ X sites. Both s and d vary with time. It was assumed that whenever an X^* site disappeared due to dissolution, Eq. 4, a new X^* site immediately formed by rapid hydration and H^+ adsorption on the aluminum that was uncovered by the leaving P species. This assumption of site renewal is identical to the assumption that the total number of sites, n_T, is constant. We partially justified this latter assumption by showing that surface area did not change significantly during the course of any of the experiments. We assume, however, without proof that the density of sites, or total sites/area, also did not vary.

The expression for the time-dependent hydrogen adsorption-desorption equilibrium involving the X and X^* sites becomes:

$$s = \frac{(n_T - d)K_a[H^+]}{1 + K_a[H^+]} = s_o - \frac{dK_a[H^+]}{1 + K_a[H^+]} \tag{7}$$

The controlling rate processes were assumed to follow power law kinetics. The best correlation of experimental data with the model was found when reaction order of 1 and 2 were assumed for the X^* sites in Eqs. 4 and 5, respectively. These rate expressions become:

$$r = k_p s \tag{8}$$

for the dissolution step, Eq. 4, and

$$-\frac{ds}{dt} = k_d s^2 \tag{9a}$$

for the deactivation step, Eq. 5. The terms k_p and k_d are constants for any particular experiment but may be functions of ionic species in solution and therefore may vary with acid concentration. Integration of Eq. 9 subject to the initial condition, $s = s_o$ at $t = 0$, yields

$$s = \frac{s_o}{1 + s_o k_d t} \tag{10}$$

Combining Eqs. 8 and 10 leads to the expression for the overall dissolution process:

$$r = \frac{k_p s_o}{1 + s_o k_d t} \tag{11}$$

Results and Discussion

The concentrations of ionic species, H^+, HSO_4^-, and SO_4^- for all reactor feed solutions was calculated assuming H_2SO_4 dissociates as follows:

$$H_2SO_4 \rightarrow H^+ + HSO_4^- \tag{12}$$

$$HSO_4^- = H^+ + SO_4^- \tag{13}$$

where Eq. 12 is complete and Eq. 13 is governed by the equilibrium constant $K_{eq} = 0.012$ kmol/m^3 (Weast, 1969) at 298 K. Table 2 shows these calculated values.

Tables 3 and 4 show concentration–time data and rates of dissolution calculated by Eq. 2 for two of the continuous-flow disso-

Table 2. Ionic Species in Solutions of H_2SO_4

Init. H_2SO_4 Conc. v/v %	Equilib. Ionic Species Conc., kmol/m^3		
	$[H^+]$	$[HSO_4^-]$	$[SO_4^-]$
0.0625	0.016	0.0064	0.0048
0.125	0.029	0.0159	0.0066
0.250	0.053	0.0367	0.0083
0.625	0.123	0.1025	0.0100
2.0	0.371	0.3487	0.0113
5.0	0.912	0.8883	0.0117
10.0	1.812	1.7882	0.0118

Table 3. Continuous-Flow Dissolution Data*

Sample Time Interval s	Avg. Time of Sample s	Dissolved Al Conc. kg/m^3 × 10^3**	Est. Φ
0–7	3.5	45.3	0.76
35–45	40	21.0	0.35
65–75	70	15.8	0.26
115–125	120	12.4	0.21
185–195	190	10.9	0.18
395–405	400	6.1	0.10
595–605	600	4.8	0.08
940–960	950	2.8	0.05
1,440–1,460	1,450	1.5	0.03
1,940–1,960	1,950	1.2	0.02
2,400–2,420	2,410	1.0	0.02

*Flow rate = 1 × 10^{-6} m^3/s, $[H^+]$ = 0.371 kmol/m^3, dry bed weight = 1 × 10^{-3} kg

**By Eq. 2, numbers in this column also equal dissolution rate × 10^6, kg/s · kg bed

Table 4. Continuous-Flow Dissolution Data*

Sample Time Interval s	Avg. Time of Sample s	Dissolved Al Conc. kg/m^3 × 10^3	Dissolution Rate kg/s · kg bed × 10^6	Φ
0–7	3.5	32.4	48.6	0.80
25–35	30	14.7	22.1	0.36
40–50	45	12.2	18.3	0.30
75–85	80	9.9	14.8	0.24
125–145	135	7.4	11.2	0.19
205–225	215	5.8	8.7	0.15
260–280	270	4.9	7.4	0.12
390–410	400	3.8	5.7	0.10
630–646	638	2.4	3.5	0.06
955–975	965	1.7	2.6	0.04
1,290–1,310	1300	1.1	1.7	0.03

*Flow rate = 1.5 × 10^{-6} m^3/s, $[H^+]$ = 0.371 kmol/m^3, dry bed weight = 1 × 10^{-3} kg

lution experiments. These data show the rapid reduction in dissolution rate with time that was typical for all runs. This reduction is assumed to be the result of deactivation of the alumina surface by formation of insoluble species. We have shown in Table 1 that for all experiments, the acid concentration was sufficiently high such that ionic species H^+, HSO_4^-, and $SO_4^=$ could be considered constant across the alumina bed. The fraction of the total alumina sample that was dissolved throughout the duration of any experiment (usually 2,400 s) was less than 1.3%.

Table 5 shows that the observed decline in rate was not the result of surface area decrease. In fact, the BET surface area of the alumina increased slightly as a result of contact with acid solutions.

The time dependence of the dissolution rate is represented by Eq. 11, which can be rearranged to the following linear form:

$$\frac{1}{r} = \frac{1}{k_p s_o} + \frac{k_d}{k_p} t \tag{14}$$

Experimental data were fitted by Eq. 14. The slope of a plot of $1/r$ vs. t is the ratio of rate constants for deactivation and dissolution. The intercept is the reciprocal of the initial rate. Figures 2, 3, 4, and 5 show that such plots correlate the data reasonably well. The lines represent the result of least-squares analysis. Table 6 summarizes the results of plotting data for all runs according to Eq. 14. The value of k_d/k_p determined from the slope of each plot is relatively constant and does not exhibit a trend with respect to flow rate and acid concentration. The average value of k_d/k_p for all of the runs is 364 ± 8.4% kg bed/kg Al dissolved. The lack of a trend suggests either that the dissolution and deactivation reactions, Eqs. 4 and 5, are zero order in the dissolved ionic species in Table 2 or that both reactions are of the same order with respect to the same dissolved ionic species.

The intercept of Eq. 14 represents the reciprocal of initial dissolution rate, $k_p s_o$. Intercepts are shown in Table 6 for each of the experiments. They decrease with increasing acid concentration in accordance with theory. They tend to vary with flow rate at all constant acid concentrations, although the variation appears to be random.

Using Eq. 6, at $t = 0$ the initial rate of dissolution can be expressed as:

$$k_p s_o = \frac{k_p n_T K_a [H^+]}{1 + K_a [H^+]} \tag{15a}$$

If it is assumed that the dissolution step, Eq. 4, is zero order in dissolved ionic species concentration, the term k_p should be constant with respect to acid concentration. The initial rate expres-

Table 5. Surface Area of Alumina Samples After 20 min Contact with Acid Solution*

$[H^+]$ kmol/m³	Surface Area m²/kg × 10⁻³
0.123	260
0.371	273
1.812	259

*Surface area before contact = 250 × 10³ m²/kg

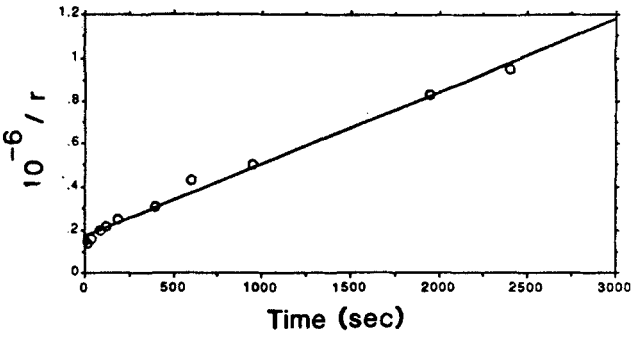

Figure 2. Dependence of dissolution rate with time.
$F = 1 \times 10^{-6}$ m³/s; $[H^+] = 0.029$ kmol/m³

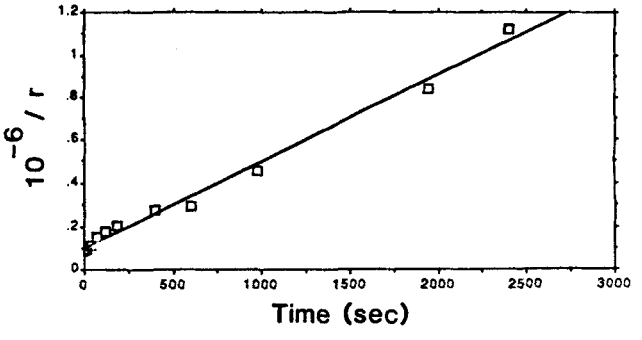

Figure 3. Dependence of dissolution rate with time.
$F = 1 \times 10^{-6}$ m³/s; $[H^+] = 0.053$ kmol/m³

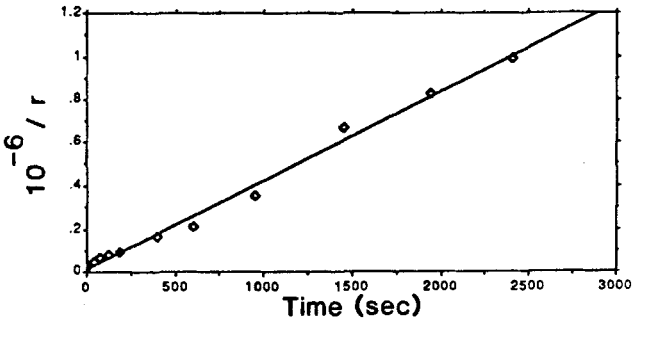

Figure 4. Dependence of dissolution rate with time.
$F = 1 \times 10^{-6}$ m³/s; $[H^+] = 0.371$ kmol/m³

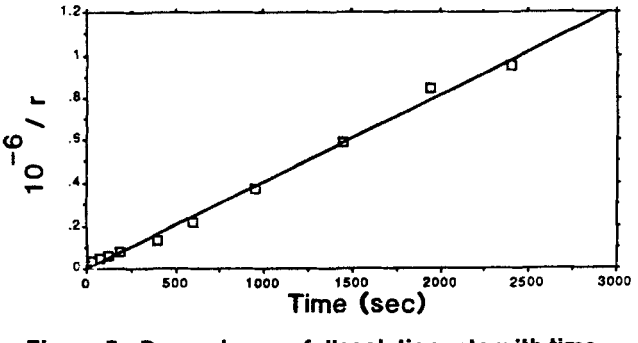

Figure 5. Dependence of dissolution rate with time.
$F = 1 \times 10^{-6}$ m³/s; $[H^+] = 0.912$ kmol/m³

Table 6. Linear Regression Parameters for Dissolution Data Fitted to Eq. 14

$[H^+]$ Conc. kmol/m³	Flow Rate m³/s × 10⁶	Intercept s · kg Al_2O_3 / kg Al × 10⁻⁴	Slope kg Al_2O_3 / kgAl	Corr. Coeff.
0.016	1.0	28.2	298	0.983
0.029	1.0	17.1	331	0.995
0.053	1.0	9.5	403	0.995
0.123	1.0	5.5	360	0.994
0.371	0.5	1.1	340	0.988
0.371	1.0	1.4	413	0.996
0.371	1.5	2.5	419	0.996
0.912	0.25	2.0	390	0.998
0.912	0.5	3.6	355	0.999
0.912	1.0	0.3	406	0.997
0.912	1.5	0.5	390	0.987
1.812	0.5	2.2	324	0.985
1.812	1.0	2.9	322	0.995
1.812	1.5	0.9	352	0.996
		Avg. slope = 364 ± 30		

sion, Eq. 15a, could then be rearranged in a linear form:

$$\frac{1}{k_p s_o} = \frac{1}{k_p n_T K_a [H^+]} + \frac{1}{k_p n_T} \tag{15b}$$

where $1/k_p s_o$ is the intercept of Eq. 14.

The open symbols and solid lines in Figure 6 show the goodness of fit of the intercept data in Table 6 to Eq. 15b. The slope and intercept of the solid line are respectively 4,400 ±170 and 12,200 ±10,800 with a correlation coefficient of 0.991. These values correspond to the following parameters in Eq. 15b:

$$K_a = 2.8 \text{ m}^3/\text{kmol}$$
$$k_p n_T = 8.2 \times 10^{-5} \text{ kg Al/s} \cdot \text{kg bed}$$

The standard error in the intercept, however, indicates that there is considerable uncertainty in the parameter values.

The parameters K_a, $k_p n_T$, and k_d/k_p can be used to estimate

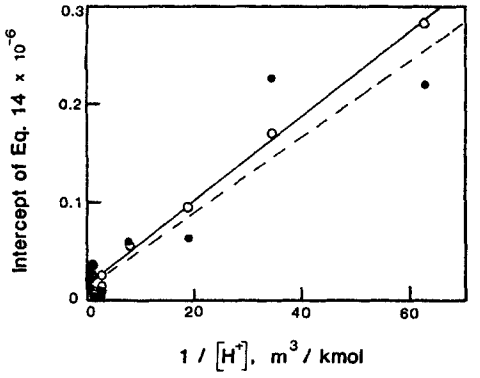

Figure 6. Langmuir plot of intercept of Eq. 14, kg bed · s/kg Al.
○, —— All data
●, --- All data for which $\phi < 0.3$

rates of the molecular processes occurring on the alumina surface. The following analysis applies to the alumina surface prior to the formation of any insoluble species.

Equation 6 suggests that in these experiments the fraction of X^* sites, s_o/n_t, varied from 0.04 to 0.84. Table 7 shows the range of acid concentrations used in this work. With reference to Eq. 15, at very high acid concentrations, the term $k_p n_T$ can be considered the initial rate of dissolution for a surface saturated with X^* sites. If, in that case, the concentration of aluminum atoms on the surface of alumina were assumed to be 8.5×10^{18} atoms/m² (Anderson, 1975; Gates et al., 1979, the turnover number would be

$$k_p' = 8.6 \times 10^{-4} \frac{\text{kmol } P}{\text{s} \cdot \text{kmol } X^* \text{ sites}}$$

for the dissolution process. Since the dissolution process is first order in X^*, this turnover number would apply at all acid concentrations and at all levels of surface deactivation. A turnover number can also be expressed in units of kmol $P/(s \times$ kmol total surface aluminum) by multiplying k_p' by the fraction of X^* sites, or s_o/n_T.

At $t = 0$, the alumina surface undergoes deactivation according to Eq. 9, which can be rearranged as follows:

$$-\frac{1}{s_o}\frac{ds}{dt}\bigg|_o = k_d s_o \tag{9b}$$

The turnover number, $k_d s_o$, expresses the kmol of insoluble surface species D per second per kmol of X^* sites. Since the deactivation process is second order, $k_p s_o$ depends upon $[H^+]$ and can be found from the experimentally determined parameter values, $k_p n_T$ and k_d/k_p, as follows:

$$k_d s_o = 364 \times (k_p n_T) \times (s_o/n_T)$$
$$= 2.9 \times 10^{-2} \times s_o/n_T, \quad \frac{\text{kmol } D}{\text{s} \cdot \text{kmol } X^*}$$

Table 7 lists these calculated values as well as the ratios of turnover numbers for deactivation and dissolution at $t = 0$ for each acid concentration studied. Turnover numbers that express the fraction of total sites deactivated per second can be found by multiplying $k_d s_o$ by the fraction of surface sites converted to X^*.

Comments on start-up and mass transfer effects

In Figures 2 through 5, the data near $t = 0$ deviate from the linear trend of the rest of the data. This deviation may result from mixing or mass transfer effects during start-up as the acid solution begins to flow through the plug and diffuses into pores of the alumina that are partially water filled. This effect was not accounted for in developing the kinetic model. The model assumes that H^+ adsorption-desorption equilibrium exists throughout all alumina particles for all t including $t = 0$.

Holdren and Berner (1979) have reported that extremely high initial dissolution rates are often the result of the dissolution of ultrafine ($\ll 1$ μm) particles that are produced during grinding of solid samples. Their samples, however, had very low surface areas (<100 m²/kg) compared to 250,000 m²/kg for the samples used in this study. We examined crushed alumina by

Table 7. Concentration of X^* Sites; Turnover Numbers for Surface Processes

$[H^+]$ kmol/m^3	s_o/n_T kmol X^* / kmol total sites	$k'_p \times 10^4$ kmol P / s · kmol X^* sites	$k_d s_o \times 10^3$ kmol D / s · kmol X^* sites	$k_d s_o/k'_p$ at $t = 0$ kmol D / kmol P
0.016	0.04	8.6	1.2	1.4
0.029	0.08	8.6	2.3	2.7
0.053	0.12	8.6	3.5	4.1
0.123	0.26	8.6	7.5	8.7
0.371	0.51	8.6	14.8	17.2
0.912	0.72	8.6	20.9	24.3
1.812	0.84	8.6	24.4	28.4
∞	1.0	8.6	29.0	33.7

scanning electron microscopy after it had been washed for 15 min in the reactor by flowing water. We found that some regions of the external surface contained fine particles with an average diameter of 0.1 μm. Some regions were clean. We estimated that these fine particles contributed at most about 0.003% to the overall surface area. Therefore, we believe the contribution of these particles to our results is insignificant.

We examined all of the dissolution data to determine the influence of diffusional effects on the observed rate after adsorption-desorption of H^+ had been established. For this determination we used the Weisz-Prater criteria (Froment and Bischoff, 1979),

$$\Phi = \frac{(-R_{H^+})L^2}{D_e[H^+]} \ll 1 \tag{16}$$

Since the consumption of H^+ could not be measured in these experiments we assumed, based upon Eq. 1, that the rate of H^+ consumption, $(-R_{H^+})$ kmol/m$^3_{\text{particle}}$ · s, was three times the rate of aluminum dissolution. Using the known particle density, 1,420 kg/m^3, we determine the relation

$$-R_{H^+} = 158 \cdot r \tag{17}$$

We estimated a diffusion coefficient for H^+ in solution as $D = 2 \times 10^{-9}$ m^2/s by the Nernst-Haskell equation (Reid et al., 1977). For this calculation HSO_4^- was assumed to be the predominant anion. An effective diffusivity, $D_e = 6 \times 10^{-10}$ m^2/s, was calculated by the equation.

$$D_e = \frac{D\epsilon}{\tau} \tag{18}$$

using the known particle pore fraction, $\epsilon = 0.6$, and an assumed tortuosity, $\tau = 2$.

We assumed the particles to be spheres and estimated the length parameter as

$$L = \frac{\text{radius}}{3} = \frac{4.6 \times 10^{-4}}{3} = 1.53 \times 10^{-4}\ \text{m} \tag{19}$$

These values led to the working expression,

$$\Phi = 6{,}160\left(\frac{r}{[H^+]}\right) \tag{20}$$

In assessing experimental data we considered values of $\Phi \leq 0.3$ as an indication that diffusional limitations were insignificant. Tables 3 and 4 show values of Φ estimated by Eq. 20 at each sample time. The two data points at early times in each table appear to have significant diffusional limitation.

We eliminated all diffusion-limited data from all experiments and fitted the remaining data to Eq. 14. Table 8 contains linear regression parameters for each experiment. The slopes in Table 8 have not changed significantly from those shown in Table 6. Some of the intercepts in Table 8 are quite different from those in Table 6; however, the plot in Figure 6 of the intercepts in Table 8 vs. $1/[H^+]$ (solid points, broken line) has not deviated significantly from the plot of intercepts from Table 6. The slope and intercept of the broken line in Figure 6 are respectively 3,900 ±450 and 12,900 ±29,000 with a correlation coefficient of 0.929. Therefore, the removal of the diffusion-limited data has

Table 8. Linear Regression Parameters for Dissolution Data Fitted to Eq. 14*

$[H^+]$ Conc. kmol/m^3	Flow Rate m^3/s ($\times 10^6$)	Intercept s · kg Al_2O_3 / kg Al $\times 10^{-4}$	Slope kg Al_2O_3 / kg Al	Corr. Coeff.
0.016	1.0	22.0	335	0.990
0.029	1.0	22.6	298	0.995
0.053	1.0	6.3	420	0.993
0.123	1.0	5.8	358	0.990
0.371	0.5	0.3	409	0.995
0.371	1.0	0.8	416	0.995
0.371	1.5	2.5	420	0.995
0.912	0.25	2.0	388	0.999
0.912	0.5	3.6	406	0.998
0.912	1.0	0.1	406	0.997
0.912	1.5	−0.01	390	0.997
1.812	0.5	2.1	322	0.992
1.812	1.0	2.9	324	0.997
1.812	1.5	0.9	350	0.998
			Avg. slope = 373 ± 36	

*All data for which $\Phi > 0.3$ were excluded from the analysis.

yielded a poorer fit of the data to model; however, the model parameters have not changed significantly.

Conclusions

The results of our experiments can be explained by a simple model that involves rapid hydration of the alumina surface, rapid adsorption-desorption equilibrium of H^+ to form a precursor surface species X^*, followed by rate-determining reactions of X^* to form dissolved aluminum and an insoluble surface species that protects the surface from further dissolution. The model also involves renewal of an X^* site each time the dissolution step occurs.

Results of kinetics experiments suggest that the dissolution and deactivation processes are respectively first and second order with respect to the X^*. The results also suggest either that the dissolution and deactivation reactions, Eqs. 4 and 5, are zero order with respect acid ions, or that both reactions are of the same order with respect to the same ionic species.

A kinetic model based upon the above mechanism adequately correlates experimental dissolution and deactivation data for continuous-flow experiments over the acid concentration range 0.0625 to 10 v/v%. Turnover numbers show that the dissolution process involves the dissolution of 8.6 atoms of aluminum per second per 10,000 X^* sites. The ratio of rates of deactivation and dissolution increases with the number of X^* surface sites.

Intraparticle mass transfer limitations affected initial rates; however, these effects had very little influence on values of model parameters determined from the experimental data.

Notation

C = dissolved aluminum concentration, kg/m^3
d = numbers of D sites/kg at $t = t$
D_e = effective diffusitivity, m^2/s
F = flow rate of acid solution, m^3/s
$[i]$ = concentration of species i, kmol/m^3
K_a = H^+ adsorption-desorption constant, m^3/kmol
k_d = second-order deactivation rate constant, kg bed/s · site
k_p = dissolution rate constant, kg dissolved Al/s · site
k'_p = dissolution turnover number, kmol dissolved Al/s · site
L = particle length parameter, m
n_T = total number of surface aluminum sites/kg
r = rate of dissolution, kg Al/s · kg bed
r_o = initial rate of dissolution, kg Al/s · kg bed
s = number of X^* sites/kg at $t = t$
s_o = number of X^* sites/kg prior to deactivation
W = weight of alumina bed, kg
$-R_{H^+}$ = rate of reaction of H^+ kmol/s · $m^3_{particle}$
Φ = Weisz-Prater number
ϵ = particle pore fraction

Literature Cited

Anderson, J. R. *Structure of Metal Catalysts,* Academic Press, New York (1975).

Chou, L., and R. Wollast, "Steady-State Kinetics and Dissolution Mechanisms of Albite," *Am. J. Sci.*, **285,** 963 (1985).

Christian J. W., *The Theory of Transformation in Metals and Alloys,* 1st ed., Pergamon, New York, 471 (1965).

Diggle, J. W., T. C. Downie, and C. W. Goulding "The Dissolution of Porous Oxide Films on Aluminum," *Electrochim. Acta,* **15,** 1079 (1970).

Dutrizac, J. E., and R. J. C. MacDonald "Ferric Ion as a Leaching Medium," *Mineral Sci. Eng.*, **6**(2), 59 (1974).

Franke, M. "An Investigation of the Kinetics and Mechanisms in the Dissolution of Alumina in Aqueous Sulfuric Acid," M.S. Thesis, Georgia Inst. Technol. (1985).

Franke, M. D., W. R. Ernst, and A. S. Myerson, "Kinetics of Dissolution of Alumina in Acidic Solution" *AIChE J.*, **33**(2), 267 (1987).

Froment, G. F., and K. B. Bischoff, *Chemical Reactor Analysis and Design,* Wiley, New York, 192 (1979).

Ganguli, P. S. "Catalyst Regeneration Process Including Metal Contaminants Removal," US Pat. No. 4,454,240 (1984).

Gates, B. C., J. R. Katzer, and G. C. A. Schuit, *Chemistry of Catalytic Processes,* McGraw-Hill, New York (1979).

Gorichev, I. G., N. G. Klyuchnikov, Z. P. Bibikova, and L. F. Popova, "Kinetics of the Dissolution of Iron (III) Oxide in Sulphuric Acid," *Zhurnal Fizicheskoi Khimii* (Engl. trans.), **50,** 1189 (1976).

Grabmaier, J., ed., *Crystals,* **8**: *Silicon-Chemical Etching,* Springer (1982).

Hernandez, J. O. "One of the Uses of Spent Hydrodesulfurization Catalysts," *Symp. Recovery of Spent Catalysts Prepr.*, Amer. Chem. Soc. Meet., Kansas City, MO, 679 (Sept., 1982).

Holdren, G. R., Jr., and R. A. Berner, "Mechanism of Feldspar Weathering. I: Experimental Studies," *Geochim. et Cosmochim. Acta,* **43,** 1161 (1979).

Holdren, G. R., Jr., and P. M. Speyer, "pH-Dependent Changes in the Rates and Stoichiometry of Dissolution of an Alkali Feldspar at Room Temperature," *Am. J. Sci.*, **285,** 994 (1985).

Hulbert, S. F., and D. E. Huff, "Kinetics of Alumina Removal from a Calcined Kaolin with Nitric, Sulphuric, and Hydrochloric Acids," *Clay Minerals,* **8,** 337 (1970).

Kabai, J., "Determination of Specific Activation Energies of Metal Oxides and Metal Oxide Hydrates by Measurement of the Rate of Dissolution," *Acta Chim. Acad. Sci. Hungaricae,* **78**(1), 57 (1973).

Maatman, R. W., P. Mahaffy, P. Hoekstra, and C. Addink "The Preparation of Pt-Alumina Catalyst and Its Role in Cyclohexane Dehydrogenation," *J. Catalysis,* **23,** 105 (1971).

Mandelbaum, P., ed., *Acid Rain: Economic Assessment,* Plenum, New York (1984).

Myerson, A. S., and W. R. Ernst, "Removal of Inorganic Contaminants from Catalysts," US Pat. No. 4,559,313 (1985).

Reid, R. C., J. M. Prausnitz, and T. K. Sherwood, *The Properties of Gases and Liquids,* 3d ed., McGraw-Hill, New York, 591 (1977).

Santacessaria, E., S. Carra, and I. Adami, "Adsorption of Hexachloroplatinic Acid on γ-Alumina," *Ind. Eng. Chem. Prod. Res. Dev.*, **16**(1), 41 (1977).

Shyr, Y-S., and W. R. Ernst, "Preparation of Nonuniformly Active Catalysts," *J. Catalysis,* **63,** 425 (1980).

Warren, I. H., and E. A. Devuyst, "Fundamentals of the Leaching of Simple Oxides," *Ind. Chem. Eng. Ser. No.* **42,** 7.1 (1974).

Weast, R. C., ed., *CRC Handbook of Chemistry and Physics,* CRC Press, Boca Raton, FL, D-91 (1969).

Manuscript received June 14, 1987, and revision received July 19, 1988.